Development 137, 2177-2186 (2010) doi:10.1242/dev.050781

The *Drosophila* serine protease homologue Scarface regulates JNK signalling in a negative-feedback loop during epithelial morphogenesis

Raphaël Rousset[1], Sophie Bono-Lauriol[1], Melanie Gettings[1], Magali Suzanne[2], Pauline Spéder[3] and Stéphane Noselli[1,*]

SUMMARY

In *Drosophila melanogaster*, dorsal closure is a model of tissue morphogenesis leading to the dorsal migration and sealing of the embryonic ectoderm. The activation of the JNK signal transduction pathway, specifically in the leading edge cells, is essential to this process. In a genome-wide microarray screen, we identified new JNK target genes during dorsal closure. One of them is the gene *scarface* (*scaf*), which belongs to the large family of trypsin-like serine proteases. Some proteins of this family, like Scaf, bear an inactive catalytic site, representing a subgroup of serine protease homologues (SPH) whose functions are poorly understood. Here, we show that *scaf* is a general transcriptional target of the JNK pathway coding for a secreted SPH. *scaf* loss-of-function induces defects in JNK-controlled morphogenetic events such as embryonic dorsal closure and adult male terminalia rotation. Live imaging of the latter process reveals that, like for dorsal closure, JNK directs the dorsal fusion of two epithelial layers in the pupal genital disc. Genetic data show that *scaf* loss-of-function mimics JNK over-activity. Moreover, *scaf* ectopic expression aggravates the effect of the JNK negative regulator *puc* on male genitalia rotation. We finally demonstrate that *scaf* acts as an antagonist by negatively regulating JNK activity. Overall, our results identify the SPH-encoding gene *scaf* as a new transcriptional target of JNK signalling and reveal the first secreted regulator of the JNK pathway acting in a negative-feedback loop during epithelial morphogenesis.

KEY WORDS: Epithelial morphogenesis, JNK signalling, Dorsal closure, Genital plate rotation, *scarface*, Serine protease homologue, *Drosophila*

INTRODUCTION

The trypsin- and chymotrypsin-like (S1 family) serine proteases (SPs) are mainly represented in animals and are implicated in food digestion, blood coagulation, immune response and development. They are almost exclusively localized outside the cytoplasm to perform their function and they are synthesized with a signal peptide for secretion. In addition, SPs are usually produced in an inactive form, which is cleaved upon a signal to form a functional protease. This mechanism favours a rapid and local response to a stimulus. For example, in mammals, cascades of localised SP activities control emergency blood clotting at a wound site (Davie et al., 1991). During *Drosophila* development, dorsoventral patterning of the embryo results from an extracellular cascade involving the SPs Nudel, Gastrulation defective, Snake and Easter and leading to the activation of the Toll pathway in the ventral region (Anderson, 1998).

SPs are endopeptidases that use a serine for their catalytic activity and are characterized by the presence of the residues histidine, aspartic acid and serine (HDS) in the active site (Rawlings and Barrett, 1993). Serine protease homologues (SPHs) are also found in various animal genomes and are defined by the lack of at least one of the essential residues of the catalytic triad HDS. Only a few SPHs have been characterized. One well-known example in mammals is the Hepatocyte growth factor or Scatter factor (HGF, SF) (Nakamura et al., 1989). In *Drosophila*, almost 30% of the 204 identified SP genes encode SPHs that are therefore most probably catalytically inactive (Ross et al., 2003; Shah et al., 2008). Only four of these SPH genes have been assigned a function. Mutations in *masquerade* (*mas*) lead to defects in somatic muscle attachment and in the formation of the nervous system during embryogenesis (Murugasu-Oei et al., 1996; Murugasu-Oei et al., 1995). The other three genes, *spheroide*, *sphinx1* and *sphinx2*, were identified in an RNAi screen aimed at identifying genes involved in immunity (Kambris et al., 2006).

We isolated the SPH encoding gene *scarface* (*scaf*) in a microarray screen designed to identify new genes transcriptionally regulated by the JNK (c-Jun N-terminal kinase) pathway during dorsal closure (DC) of the *Drosophila* embryo. DC is a major morphogenetic movement that takes place after germ-band retraction to close the eye-shaped opening of the dorsal embryonic epidermis, over the transient tissue called the amnioserosa (AS). Cell elongation is responsible for the dorsalward spreading of the lateral epithelial sheets. The AS, conversely, progressively reduces through cell constriction and engulfment accompanied by cell death (Franke et al., 2005; Kiehart et al., 2000; Reed et al., 2004). Precise activation of the JNK pathway, specifically in the dorsal-most row of epithelial cells in contact with the AS (the leading edge, LE), is a prerequisite for DC progression (Bates et al., 2008;

[1]University of Nice Sophia-Antipolis, UMR 6543 CNRS, Institute of Developmental Biology and Cancer, Parc Valrose, 06108 Nice CEDEX 2, France. [2]Howard Hughes Medical Institute, Laboratory of Apoptosis and Cancer Biology, The Rockefeller University, 1230 York Avenue, New York, NY 10065, USA. [3]The Wellcome Trust/Cancer Research UK Gurdon Institute, University of Cambridge, Tennis Court Road, Cambridge CB2 1QN, UK.

*Author for correspondence (noselli@unice.fr)

Accepted 27 April 2010

Byars et al., 1999; Glise et al., 1995; Glise and Noselli, 1997; Martin-Blanco et al., 1998; Reed et al., 2001). Several transcriptional targets of the JNK pathway have already been described during DC, such as the profilin-coding gene *chickadee*, the transcription factor *cabut*, the integrin-coding genes *scab* and *myospheroid* or the trafficking gene *Rab30* (Homsy et al., 2006; Jasper et al., 2001; Munoz-Descalzo et al., 2005; Thomas et al., 2009). However, only two target genes are specifically expressed in the LE, *decapentaplegic* (*dpp*) and *puckered* (*puc*) (Glise et al., 1995; Glise and Noselli, 1997). Dpp, of the TGFβ family, participates in cell spreading of the lateral epithelium, cell constriction in the AS and connection of these two tissues (Fernandez et al., 2007; Wada et al., 2007). Dpp also regulates remodelling of the cytoskeleton in the segment border cells by activating Cdc42 and dPak (Ricos et al., 1999). The gene *puc* encodes a phosphatase that sets up a negative-feedback loop at the level of the c-Jun kinase Basket (Bsk) (Martin-Blanco et al., 1998). In addition, other JNK target genes are involved in different biological processes. For instance, JNK-induced expression of matrix metalloproteinases is required for disc eversion and tumour invasion (Srivastava et al., 2007); JNK protection against oxidative stress is realized through expression of autophagy-related genes (Wu et al., 2009); and during immune response, JNK participates in the expression of antimicrobial peptide genes (Delaney et al., 2006).

In this paper, we report the characterization of *scaf* during *Drosophila* development. The catalytic triad of the SP domain of Scaf lacks two of the conserved HDS residues and Scaf was thus classified as a SPH (Ross et al., 2003). Although a previously isolated semi-lethal mutation led to adult escapers exhibiting a head scar under the proboscis (Bonin and Mann, 2004), no function has been attributed to *scaf*. Here we show that the JNK signalling pathway regulates *scaf* expression in the embryo and in imaginal discs. In S2 cells and in vivo, the protein Scaf is secreted, indicating that it behaves as an extracellular SPH. Loss-of-function and gain-of-function in vivo studies uncovered an essential role of *scaf* during epithelial morphogenesis through antagonistic regulation of JNK signalling.

MATERIALS AND METHODS

Fly stocks

The following fly lines were used: *en-GAL4^{e16E}* (gift from A. Brand, University of Cambridge, UK), *AbdB-GAL4* (gift from E. Sanchez-Herrero, Universidad Autónoma de Madrid), *ptc-GAL4* (gift from N. Perrimon, Harvard Medical School, USA), *UAS-dpp* (gift from K. Basler, University of Zurich, Switzerland), *UAS-hep^{4E}* (WT), *hep^{1}* and *hep^{r75}* (Glise et al., 1995), *puc^{E69}* (*puc-lacZ*) (Ring and Martinez Arias, 1993), and *UAS-puc2A* (Martin-Blanco et al., 1998). The following lines from Bloomington were also used: *w^{1118}* (#3605), *69B-GAL4* (#1774), *act-GAL4* (#4414), *pnr-GAL4* (#3039), *UAS-hep^{act}* (#9306), *UAS-EGFP* (#5431), *UAS-CD8GFP* (#5137), *UAS-p35* (#5072), *CyO,Kr-GAL4,UAS-GFP* balancer (#5194) (Casso et al., 2000), and Δ*scaf* deficiency (#8884); as well as *UAS-scafRNAi* (#13249) and *UAS-Dicer2* (#60009) from VDRC.

scaf cDNA was obtained from the EST GH05918 (DGRC). The following recombinants were created for this study: (1) Rescue – *scaf* (*scaf^{f01332}*, *scaf^{PBss}* or *scaf^{11}*),*act-GAL4* and *scaf* (*scaf^{11}*, *scaf^{PBss}* or *scaf^{11}*),*UAS-scaf*; (2) RNAi – *UAS-scafRNAi,UAS-Dicer2*; and (3) Q-PCR – *pnr-GAL4,puc^{E69}*. The recombinants for the rescue were balanced with *CyO,Kr-GAL4,UAS-GFP*. We also made the following stocks: (1) overexpression in the disc (Fig. 4F) – *ptc-GAL4;puc^{E69}//SM6a;TM6B*; (2) overexpression in the disc (Fig. 7A) – *UAS-EGFP;UAS-puc2A* and *UAS-scaf;UAS-puc2A*; and (3) live imaging – *UAS-CD8GFP/SM5;AbdB-GAL4/TM6B*. The majority of the crosses were done at 25°C, the others were carried out at 29°C as indicated in the text.

scaf alleles

scaf^{f01332} (Exelixis) and *scaf^{PBss}* (Bonin and Mann, 2004) correspond to PiggyBac insertions. We used *scaf^{KG05129}* (Bloomington #13631) as a starter line for imprecise P element jump events by action of a P transposase. Two white minus lethal lines were selected: *scaf^{11}* and *scaf^{27}*. Deletions were mapped by PCR on genomic DNA and sequencing.

The lethality associated with the *scaf* zygotic loss-of-function was determined as follows: eggs were collected at 25°C from *CyO,Kr-GAL4,UAS-GFP* balanced *scaf* lines or from the crosses *scaf,act-GAL4/CyO,Kr-GAL4,UAS-GFP* × *scaf,UAS-scaf/CyO,Kr-GAL4,UAS-GFP* for the rescue experiments. Ten hours after egg laying (AEL), GFP-minus dechorionated embryos were raised at 25°C, covered with Voltalef oil (Prolabo). We collected larvae that hatched and made cuticle preparations from the remaining dead embryos. We let the larvae grow to determine if they die during the larval or pupal stage, and if they give rise to some escapers. Experiments were done in parallel with a *w^{1118}* line and we performed a statistical analysis (Student's *t*-test) on the different stages of lethality.

Microarray screen

We used the Affymetrix DNA microarrays (DrosGenome1) to identify genes whose expression is regulated by the JNK pathway. Two genetic conditions were compared, wild-type and gain-of-function embryos, in which the JNK pathway is strongly activated by expressing Hep^{act} in the ectoderm using the UAS-GAL4 system (*69B-GAL4*). This allowed us to isolate 634 JNK target genes that are activated by a fold change of at least 1.8. Present among these genes were *puc* with a fold change of 2.0 and *scaf* with a fold change of 1.8. A secondary screen based on in situ hybridization led to the validation of *scaf*, as well as several other genes (R.R., F. Carballès and S.N., unpublished data). Microarray data have been deposited in the Gene Expression Omnibus (accession number GSE21805).

In situ hybridization

Digoxigenin (DIG)-labelled RNA probe synthesis and in situ hybridization (ISH) experiments were performed using a standard protocol. Anti-DIG antibody conjugated to alkaline phosphatase (1/2000; Roche Diagnostics) was used and revelation was performed with NBT/BCIP reagent (Sigma). For fluorescent ISH coupled to immunostaining, the second fixation step was performed using freshly prepared paraformaldehyde and proteinase K treatment was not done. Primary antibodies were: rabbit anti-Scaf2 (1/50) and mouse anti-Ena (1/50). Sheep anti-DIG antibody coupled to horseradish peroxidase (1/2000; Roche Diagnostics) was joined to the secondary antibodies anti-rabbit Al488 (1/400; Molecular Probe) and anti-mouse Cy5 (1/100; Jackson ImmunoResearch). Revelation was done twice for 30 minutes with Tyramide Signal Amplification (PerkinElmer). Embryos were mounted in Mowiol 4-88 Reagent (Calbiochem).

Scaf antibodies

We raised polyclonal antibodies against two different GST fusion proteins containing Scaf residues 138-270 (Scaf1 antibody) or 297-408 (Scaf2 antibody). Approximately 1 mg of the proteins was injected into a New Zealand White rabbit. The sera were affinity-purified on His-tagged peptide columns (Affi-gel 10; Bio-Rad) according to the manufacturer recommendations, except that we used the ImmunoPure Gentle Ag/Ab elution buffer pH 6.55 (Pierce). Finally, we tested the affinity-purified Scaf antibodies by western blotting and by immunostaining to ensure specificity.

Immunostainings

Embryos were prepared as described for ISH and the incubation buffer was 0.1% PBS-Triton X-100 with 1% BSA. The following primary antibodies were used: rabbit anti-Scaf1 and 2 (1/200); mouse anti-En 4D9 (1/500; ascites fluid; DSHB); mouse anti-Ena 5G2 (1/500; DSHB); mouse anti-Lamin (1/50; DSHB); rat anti-Troponin H (1/300; Babraham Tech) and mouse anti-Golgi (1/500; Calbiochem). Nuclear staining was done with DAPI (10 μg/ml, Biochemika). For the actin staining, we used methanol-free formaldehyde (Polysciences, Inc.) in the fixation step and devitellinization was performed without methanol. We used instead chilled 80% ethanol. Actin was labelled with FluoProbes 547H or 647H phalloidin

(Interchim). For the soft protocol, embryos were prepared as described above for the actin staining. In addition, the buffer did not contain Triton X-100, but Tween-20.

The genital discs were dissected from male L3 larvae in distilled water, transferred into cold PBS and fixed with 4% formaldehyde. Immunostaining was performed in 0.1% PBS-Triton X-100 and 1% BSA. We used the rabbit anti-Scaf2 (1/200) or the rabbit anti-En (1/200; Santa Cruz) and the chicken anti-βgalactosidase antibody (1/1000; Genetex).

S2 cell experiments

S2 cells were transfected using the Effectene reagent (Qiagen). For overexpression experiments, we co-transfected a DNA mix made of pAct-GAL4 and pUAS-*scaf* or pUAS-*scaf*GFP for about 24 hours. For RNAi experiments, we transfected 16 µg of double-stranded RNA directed against GFP or *Syx5* in 1 ml of minimal Schneider's medium at 22°C for 1 hour. We then added 2 ml of complete medium and left the cells for 5 days at 22°C. Cell lysates were obtained by incubating S2 cells with RIPA solution containing a protease inhibitor cocktail.

For western blotting, we loaded 80 µg of proteins coming from the cell lysates and 25 µl of culture supernatant. We used the rabbit anti-Scaf2 or the rabbit anti-Scaf1 (1/700) and the mouse anti-βTub (1/200, DSHB). Revelation was performed with the Immobilon Western reagent (Millipore).

The Multigauge V2.3 program (Fujifilm) was used for signal quantification on the western blot. Quantification is based on pixel intensity. For each lane of the lysates, the background was subtracted to the signal intensity of the band of interest and of the βTub loading control, and the ratio of these two values was calculated.

Cuticle preparations

Embryos were collected for 24 hours and incubated at 25°C to let the wild-type larvae crawl away. The cuticles of unhatched (dead) embryos were prepared using a standard protocol.

Quantitative PCR

Embryos from *pnr-GAL4,pucE9/TM6B* flies crossed to w^{1118}, *UAS-hep*^{act} or *UAS-scafRNAi,UAS-Dicer2* homozygotes were collected at 25°C or 29°C. They were dechorionated, frozen in liquid nitrogen and stored at –80°C. They were then lysed with the TissueLyser LT (Qiagen) and RNA was extracted with the RNeasy Mini Kit (Qiagen). Reverse-transcription was performed with SuperScript III Reverse Transcriptase (Invitrogen) after DNase I digestion with a mix of oligo-dT and random primers. The following primers were used: CTTCATCCGCCACCAGTC (forward) and CGACGCACTCTGTTGTCG (reverse) for the endogenous control *rp49*, and GGTTACGATGCGCCCATCTA (forward) and ACGGCGGA-TTGACCGTAAT (reverse) for *lacZ*. Q-PCR was performed with the Mastermix Plus for SYBR Green containing Rox (Eurogentec) and standard curves showed a 100% efficacy for *rp49* amplification and 99% for *lacZ*. For each condition we did three biological and four technical replicates. Results were analysed with the StepOne software v2.1 (Applied Biosystems).

Time lapse

To follow the genitalia rotation in vivo, male pupae were selected at the prepupal stage (0-12 hours after puparium formation) and incubated at 25°C or 29°C for 24 hours. The most-posterior part of the pupae was then cut in water. The pupae were stuck upside down in an agar plate and covered with water. Acquisitions of a *z*-stack (around 150-200 mm depth) were taken every 15 minutes over 15 hours with a Zeiss LSM 510 Meta confocal microscope.

RESULTS

scaf is a novel JNK target gene in the LE during DC

We carried out a genomic analysis of JNK target genes during DC using the Affymetrix oligo-chips (R.R., F. Carballès and S.N., unpublished data). A secondary screen using in situ hybridization (ISH) on embryos led to the validation of several candidates. We particularly focused on *scaf* because of its strong and specific expression in the LE during DC, similar to the classical JNK target gene *dpp* (Fig. 1A,E). *scaf* mRNA is first visible during germband retraction (stage 12 of development) and is detected in the LE until the end of DC (stage 16; see Fig. S1 in the supplementary material). The expression is also noticeable in some cells of the AS, in particular at the posterior canthus (Fig. 1A), as well as in the ventral ectoderm (Fig. 1I). *scaf* mRNA is no longer present in the LE of embryos mutant for *hep*, although it is still visible in the ventral ectoderm (Fig. 1B). When we overexpressed the active form of JNKK (Hemipterous, Hep^{act}) in the posterior compartment of each segment (*en>hep*^{act}), we observed the appearance of ectopic stripes of *scaf* expression overlapping these compartments (Fig. 1C). JNK signalling is thus sufficient for *scaf* expression. In order to determine whether *scaf* is a primary target of JNK or a secondary one through the activation of the Dpp pathway, we expressed *dpp* in stripes (*en>dpp*) and observed that, in these embryos, *scaf* expression is wild-type (Fig. 1D). These data indicate that *scaf* is a novel primary JNK target gene in the LE of dorsally closing embryos, like *puc* and *dpp* (Fig. 1J).

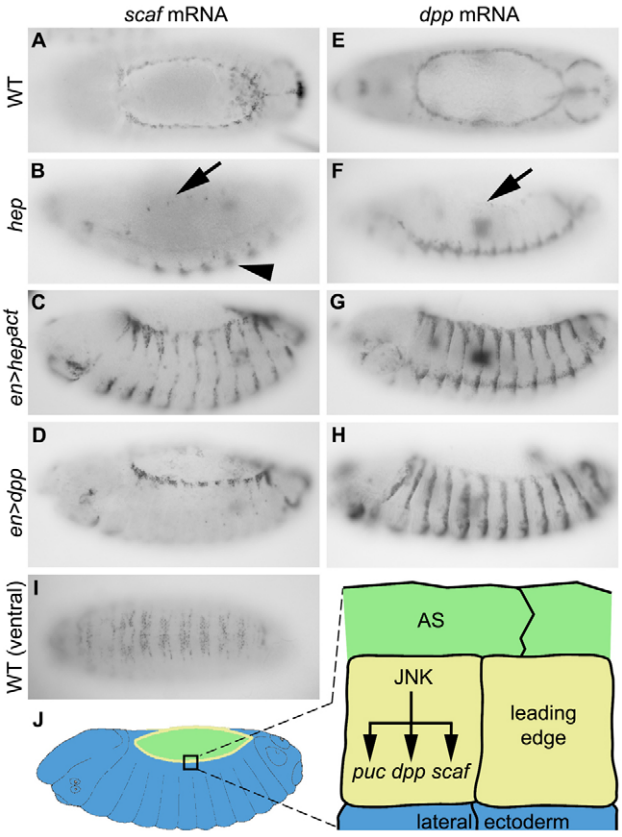

Fig. 1. JNK-induced expression of *scaf* in the LE cells during embryonic DC. (**A-I**) In situ hybridization experiments were performed to detect *scaf* mRNA (A-D,I) and the control *dpp* mRNA (E-H) in wild-type (WT) embryos (A,E,I), *hep*^{1}/*hep*^{r75} mutants (B,F), *en-GAL4/UAS-hep*^{act} (ectopic JNK activity; C,G) and *en-GAL4/+; UAS-dpp/+* embryos (ectopic Dpp activity; D,H). Arrows show the position of the leading edge (LE) in the *hep* mutants and the arrowhead shows the ventral expression, which does not depend on JNK signalling (B). Anterior is to the left (as in all following figures showing embryos). Embryos are visualized from a lateral view, except for panels A and E (dorsal) and I (ventral). (**J**) *dpp*, *puc* and *scaf* are the three known JNK target genes with a specific expression at the LE during dorsal closure (DC).

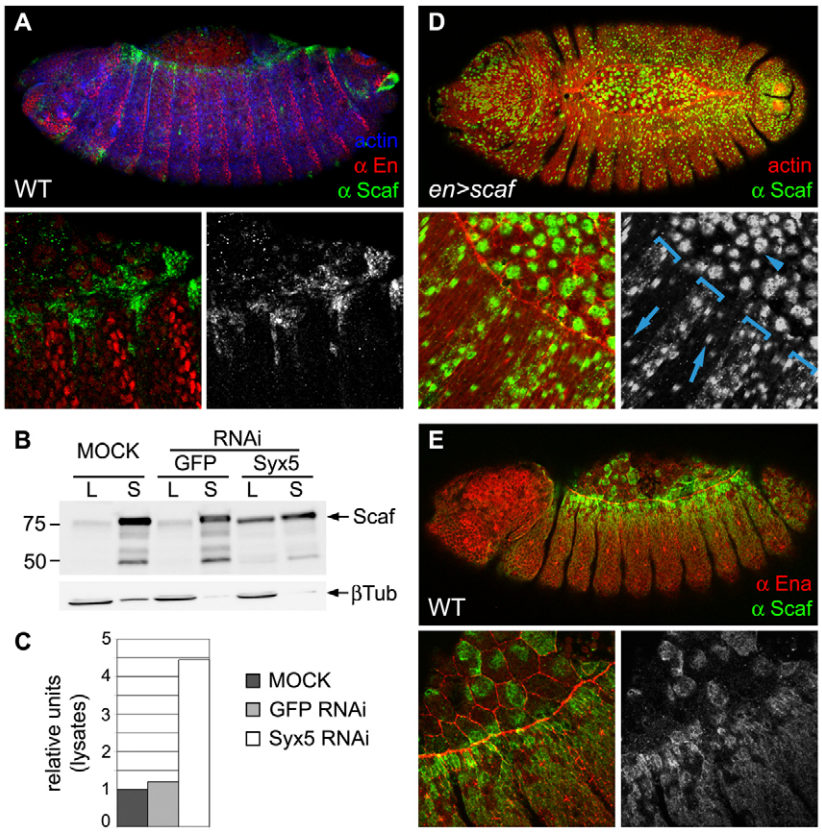

Fig. 2. Scaf protein expression and localization in the embryo. (**A**) Immunostainings (using Triton) showing Scaf expression (green; using antibody 2) at the LE of a stage-14 wild-type embryo. Blue, Actin (stained with phalloidin); red, En. The two lower panels show a close-up at the LE. Black and white panel, Scaf. The Scaf staining is absent in *scaf* mutants, demonstrating the specificity of the antibodies (see Fig. 3D). Note the non-uniform, segmented expression of Scaf at the LE, which is reduced, if not absent, in the En-positive posterior compartment of each segment. Scaf expression is also detected in some cells of the amnioserosa (AS). (**B**) Western-blots with anti-Scaf and anti-βTubulin antibodies. Endogenous Scaf is present both in the crude S2 cell lysate (L) and in the culture medium supernatant (S). Note a weak release (due to partial cell death) of the intracellular control βTubulin (lower panel) in the culture medium that does not account for the amount of secreted Scaf. Reduction of Scaf secretion was observed when cells were treated with *Syntaxin 5* (*Syx5*) double-stranded (ds) RNA, but not with the control GFP dsRNA. (**C**) Quantification of the Scaf signals (relative units in comparison with the MOCK) observed in the lysates. Increased amount of Scaf is present in the lysate of *Syx5* RNAi-treated cells, indicating a decrease of secretion. (**D**) In embryos ectopically expressing Scaf (green) in stripes with the *en-GAL4* driver, Scaf protein is present in the lateral ectoderm outside (blue arrows) of the *en*-expressing domain (which is discernible by a higher expression of Scaf; blue brackets) and in the cytoplasm of AS cells (blue arrowhead; see also Fig. S4 in the supplementary material). This non-autonomous localization is not due to a leaky activation of the parental strains (R.R., unpublished data). Red, Actin. (**E**) WT embryos stained using a soft protocol revealed the presence of endogenous Scaf outside of its expression domain. This staining is lost in a *scaf* mutant, which shows the specificity of the antibody (see Fig. S5 in the supplementary material). Red, Ena. For panels A, D and E, the same staining is obtained with anti-Scaf1 antibody (see Fig. S3 in the supplementary material) (R.R. and S.B.-L., unpublished data). A and E, lateral view; C, dorsal view.

Scaf is a secreted protein

In order to characterize the endogenous Scaf protein, we made affinity-purified antibodies directed against two distinct non-conserved regions (see Fig. S2A,B in the supplementary material). Immunostainings coupled to fluorescent ISH of wild-type embryos (using Triton) indicated that the protein was localised in the same *scaf* mRNA-expressing cells (see Fig. S2C in the supplementary material). In particular, Scaf is detected in the LE cells, with a stronger expression at both extremities (Fig. 2A). As Scaf contains a putative signal peptide, we tested the capacity of Scaf to be secreted. In S2 cells, the endogenous (Fig. 2B,C) and overexpressed (see Fig. S3C,D in the supplementary material) protein is detected in the culture medium, indicating that Scaf has indeed been secreted. Secretion is diminished when cells are treated by RNAi to silence Syntaxin 5 (Syx5), an essential protein of the secretory pathway (Fig. 2B,C) (Xu et al., 2002). In *en>scaf* embryos in vivo, the protein was detected within cells located outside the *en*-expressing cells, both in the anterior cells and in the AS cells (Fig. 2D). Co-stainings with markers of the nuclear envelope, of the endoplasmic reticulum and of the Golgi apparatus did not detect subcellular colocalization with Scaf in these cells (see Fig. S4 in the supplementary material). A similar pattern of Scaf localization outside of its expression domain, in the lateral ectoderm and the AS, was also revealed in wild-type embryos using a soft immunostaining protocol (Fig. 2E; see Fig. S5 in the supplementary material), although the signal was weaker compared with the overexpression condition (Fig. 2D). Apparent differences in stainings at the LE when comparing Fig. 2D and Fig. S2 with Fig. 2E are explained by the fact that two permeabilization protocols were used. In Fig. 2E, Triton was not used to allow detection of secreted Scaf, but this led to reduction of Scaf detection expressed at the LE. By contrast, in Fig. 2A and Fig. S2,

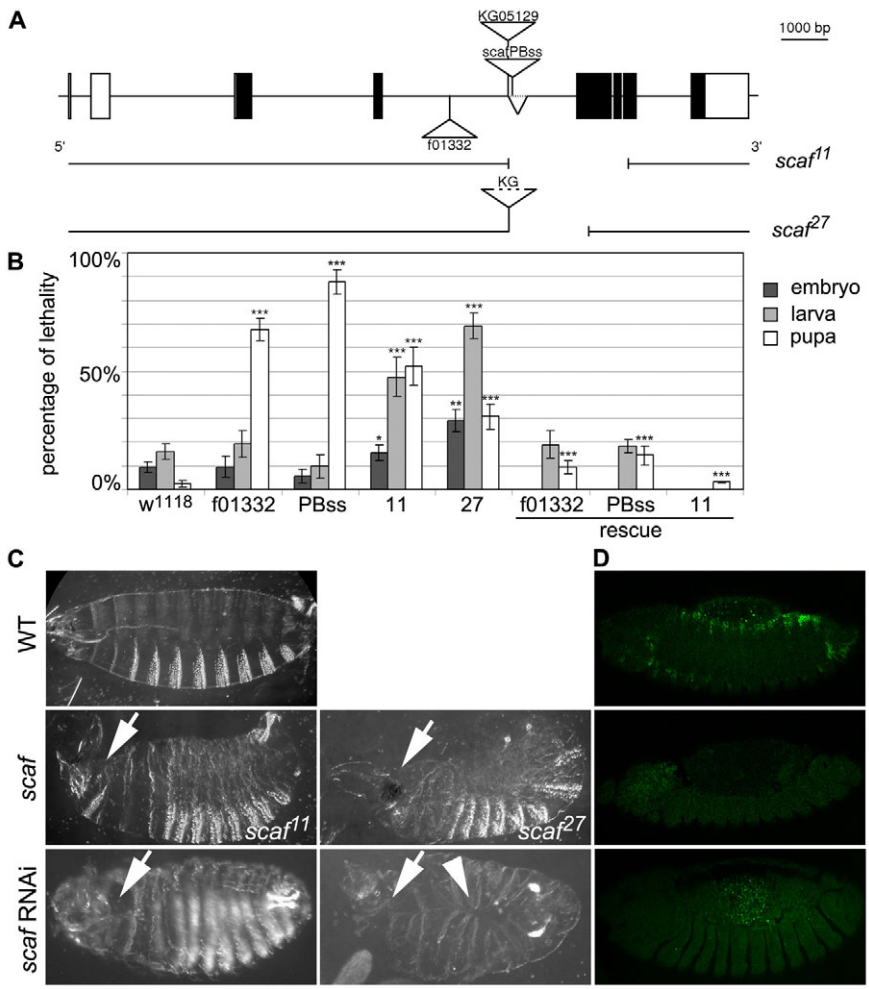

Fig. 3. *scaf* zygotic loss-of-function phenotypes in the embryo. (**A**) Genomic organization of the *scaf* locus and associated mutations. Straight lines represent the introns, white boxes represent the untranslated regions and black boxes represent the coding sequences. Lines below the locus pattern indicate the DNA lesions associated with the two white-minus alleles, $scaf^{11}$ and $scaf^{27}$, obtained by KG05129 excision. Note that in the $scaf^{27}$ strain, part of the P element is still present. Broken lines within the locus signals a missing sequence in the *KG05129* allele. (**B**) Histogram showing the percentages of lethality at different stages of development for the four *scaf* alleles, the control w^{1118} and the rescue experiments (rescue was not performed with $scaf^{27}$). s.d. was calculated for each point (error bars) and a Student's *t*-test was performed. *, P=0.05; **, P=0.01; ***, P=0.001. (**C**) Cuticles of $scaf^{11}$ (25% of the dead embryos, n=52; i.e. 4% of total homozygote embryos) and $scaf^{27}$ (40%, n=40; i.e. 12% of total homozygote embryos) zygotic mutant embryos (middle panels), as well as *scaf* RNAi embryos (*69B-GAL4/UAS-scafRNAi,UAS-Dicer*; bottom panels; 48% of penetrance at 29°C, n=372), all displaying dorsal defects compared with a WT embryo (top panel). Arrows indicate anterior openings and the arrowhead indicates dorsal puckering. (**D**) Immunostainings with anti-Scaf2 antibody show loss of Scaf expression in $scaf^{11}$ mutants (middle panel) and *scaf* RNAi embryos (bottom panel) compared with WT (top panel). We observed no signal with both anti-Scaf antibodies when staining $scaf^{11}$ and $scaf^{27}$ mutant embryos (S.B.-L., unpublished data).

Triton allowed detection of Scaf only in the LE. All together, these results indicate that Scaf is a secreted SPH both in cultured cells and in vivo, suggesting a function of Scaf in the extracellular space during DC.

scaf loss of function results in epithelial morphogenetic defects

In this study, we used four different *scaf* alleles: $scaf^{PBss}$, $scaf^{f01332}$, $scaf^{11}$ and $scaf^{27}$. $scaf^{PBss}$ and $scaf^{f01332}$ correspond to two previously described PiggyBac insertions (Bonin and Mann, 2004; Thibault et al., 2004) and we generated $scaf^{11}$ and $scaf^{27}$ from P element imprecise excision that created small deletions within the locus (see Materials and methods; Fig. 3A). Whereas $scaf^{27}$ is lethal, the other alleles are, like $scaf^{PBss}$, semi-lethal and the adult escapers bear a scar on their inferior head with no apparent other defects (Fig. 4A) (Bonin and Mann, 2004). Based on the percentage of escapers (Table 1) and the lethality during the different stages of development (Fig. 3B), we established the strength of each allele, from the weakest to the strongest, as following: $scaf^{f01332}$, $scaf^{PBss}$, $scaf^{11}$, $scaf^{27}$. Interestingly, the dead embryos corresponding to the $scaf^{11}$and $scaf^{27}$ zygotic mutants displayed cuticle phenotypes corresponding to DC defects (Fig. 3C). Indeed, we observed opening of the anterior part of the embryo ('anterior open'), as well as puckering of the dorsal cuticles that resemble defects due to JNK hyperactivity (see below). Immunostainings did not detect the Scaf protein in these embryos, indicating the loss of Scaf expression and revealing the specificity of the antibodies (Fig. 3D). Importantly, rescue experiments saved the lethality and restored cuticle formation (Fig. 3B) (S.B.-L., unpublished data), therefore proving that the observed phenotypes are due to the mutations in the *scaf* locus.

To further confirm the *scaf* loss-of-function phenotypes, we expressed a hairpin RNA corresponding to *scaf* (along with Dicer to enhance RNAi) using the epidermal driver *69B-GAL4*. *scaf* RNAi embryos resembled $scaf^{11}$and $scaf^{27}$ embryos (Fig. 3C). Efficiency of the RNAi was validated by immunostaining, which showed a loss of Scaf protein expression (Fig. 3D).

Diverse adult phenotypes were also noticed with other drivers (*ptc-GAL4* and *AbdB-GAL4*). Scars under the proboscis confirmed the correct targeting of the RNAi against *scaf* (Fig. 4A). In addition, we observed loss of wing veins and thorax mechanosensory bristles, as well as male terminalia malformations (Fig. 4B) (R.R., unpublished data). The latter phenotype is of particular interest as JNK signalling has been previously implicated in male genital plate morphogenesis (Macias et al., 2004; McEwen and Peifer, 2005; Polaski et al., 2006). *scaf* RNAi led to genitalia rotation defects and partial dissociation of the genital plate from the abdomen, indicating that the *scaf* gene also participates in male terminalia morphogenesis (Fig. 4B). In conclusion, invalidation of *scaf* function affected morphogenetic movements controlled by JNK signalling such as DC and male genitalia formation.

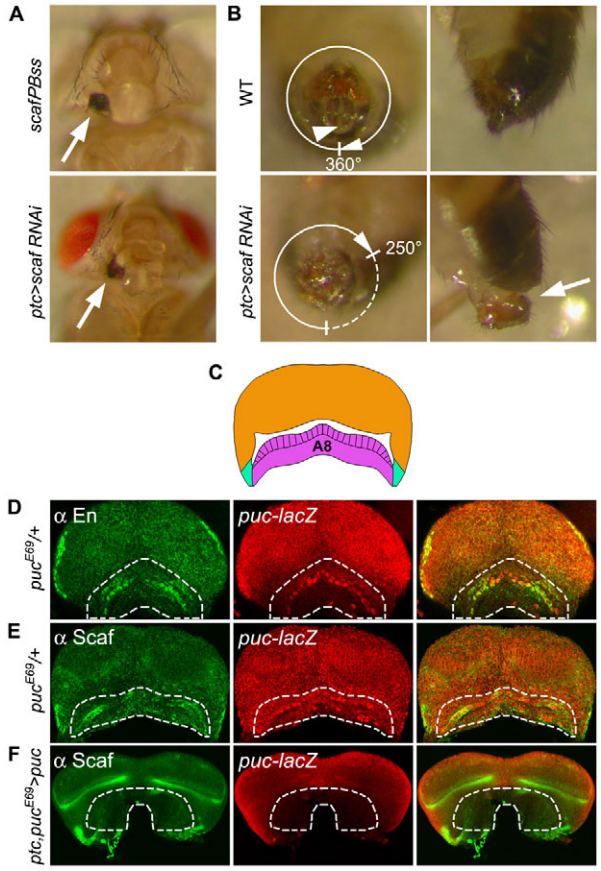

Fig. 4. *scaf* adult loss-of-function phenotypes and JNK-regulated Scaf expression in male genital discs. (**A**) Head scars (white arrows) of $scaf^{PBss}$ (top panel) and *ptc>scaf RNAi* (*ptc-GAL4/+;UAS-scafRNAi,UAS-Dicer*; bottom panel; 29°C) adult escapers. (**B**) Genital rotation defects of *ptc>scaf RNAi* adult males (bottom panels; 29°C), compared with WT (top panels). The same defects were seen with *AbdB-GAL4*. The dorsal position of the analia (arrowhead) in WT males indicates a full 360° rotation. In *ptc>scaf RNAi* adults, the analia did not reach the dorsal position, revealing an incomplete rotation of the plate. In addition, a separation of the plate from the dorsal abdomen can be observed (white arrow in the bottom right panel). (**C**) Outline of a male genital disc (ventral view). The three segments are differently coloured: pink for A8, orange for A9 and blue for A10. The posterior compartment of the A8 segment is hatched. (**D-F**) Immunostainings of control genital discs (puc^{E69}/+; D,E) and JNK loss-of-function discs (*ptc-GAL4/+;UAS-puc/*puc^{E69}; F) containing the JNK activity reporter *puc-lacZ* (puc^{E69}). The genital discs were stained with anti-En (D; green) or anti-Scaf2 (E,F; green) antibody and anti-β-Galactosidase antibody (red). The A8 is outlined with a white dotted line.

JNK signalling drives *scaf* expression in the A8 segment of the male genital disc

We decided to use the genitalia as a second model of morphogenetic tissue to study the role of *scaf* and JNK signalling. The male genital plate derives from a unique, centrally located imaginal disc, called the genital disc. Three groups of cells originally coming from the abdominal segments A8, A9 and A10 of the embryo assemble to form the complete larval disc, each primordium containing an anterior compartment and a posterior one (drawing in Fig. 4C) (Chen and Baker, 1997; Freeland and Kuhn, 1996). During pupariation, the male genital disc undergoes partial eversion and metamorphoses. The disc also turns dextrally,

Table 1. Percentage of adult escapers into the homozygous mutant populations for strains $scaf^{f01332}$, $scaf^{PBss}$, $scaf^{11}$ and $scaf^{27}$ and percentage of viable adults for the rescue experiments

Genotype	% adults	*n*
$scaf^{f01332}$	14.7% ± 0.040	436
$scaf^{PBss}$	2.6% ± 0.021	205
$scaf^{11}$	1.0% ± 0.016	228
$scaf^{27}$	–	346
$scaf^{f01332}$,*act>scaf*	71.5% ± 0.057	200
$scaf^{PBss}$,*act>scaf*	69.3% ± 0.038	37
$scaf^{11}$,*act>scaf*	23.5% ± 0.096	63

No escaper was observed in the $scaf^{27}$ strain. Percentages are ±s.d. *n* corresponds to the number of homozygous larvae that were collected.

accomplishing a full 360° rotation. We recently showed that the A8 segment is an organizer of this directional left-right morphogenesis through the activity of a novel type ID unconventional myosin (Speder et al., 2006; Speder and Noselli, 2007). We used the *puc-lacZ* reporter line to monitor the activity of JNK signalling in the male genital disc. Anti-β-Galactosidase immunostaining revealed a row of cells with a strong signal in the A8 segment (Fig. 4D), like previously reported (Macias et al., 2004). In addition, we show that this signal colocalises with the posterior determinant Engrailed (Fig. 4D). This indicates that JNK activity is high in the posterior compartment of the A8 segment. Moreover, we also detected some activity in the anterior compartment, as well as in the A9 segment. This weak staining was repressed by Puc overexpression (Fig. 4F) and thus corresponds to a basal activity of JNK signalling rather than a non-specific staining. The anti-Scaf antibody stained the same cells as the *puc-lacZ*-positive cells in the posterior A8 compartment, suggesting that *scaf* is also a JNK target gene in this tissue (Fig. 4E). Indeed, Scaf staining was lost when JNK signalling was inhibited in the A8 segment by Puc overexpression with *ptc-GAL4* (Fig. 4F). Therefore, the JNK pathway controls *scaf* expression in the male genital disc, like in the embryo.

JNK signalling controls dorsal fusion of the A8 segment extremities in the male genital disc

Previous studies based on *puc* ectopic expression revealed the involvement of JNK signalling in male terminalia formation (Macias et al., 2004; McEwen and Peifer, 2005). Consistently, mutations in *hep* (Holland et al., 1997) or the JNKKK-encoding *slipper* gene (Polaski et al., 2006) also affected male plate morphogenesis. To assess the effect of JNK inhibition in specific domains of the male genital disc, we used three different drivers to overexpress Puc: *AbdB-GAL4* (expressed predominantly in the anterior compartment of the A8 segment), *en-GAL4* (strictly in the posterior compartment) and *ptc-GAL4* (in both compartments) (Speder et al., 2006). *en-GAL4* and *ptc-GAL4* drivers, but not *AbdB-GAL4*, also drive expression in the A9 and A10 segments (Speder et al., 2006). As previously described (Macias et al., 2004; McEwen and Peifer, 2005), two types of highly penetrant phenotypes were observed: an incomplete rotation of the plate (between 70° and 359° depending on the driver) and an incomplete fusion of the genital arch (Fig. 5A,B). In contrast to *en-GAL4* and *ptc-GAL4*, which affected both processes, *AbdB-GAL4* induced misrotation without arch defect (Fig. 5A,B). Whereas rotation, as already mentioned, depends on the A8 segment, genital arch formation derives from the A9 segment of the disc (Estrada et al., 2003). This indicates a requirement of JNK in the A8 segment for rotation and in the A9 segment for arch fusion. Similar results were

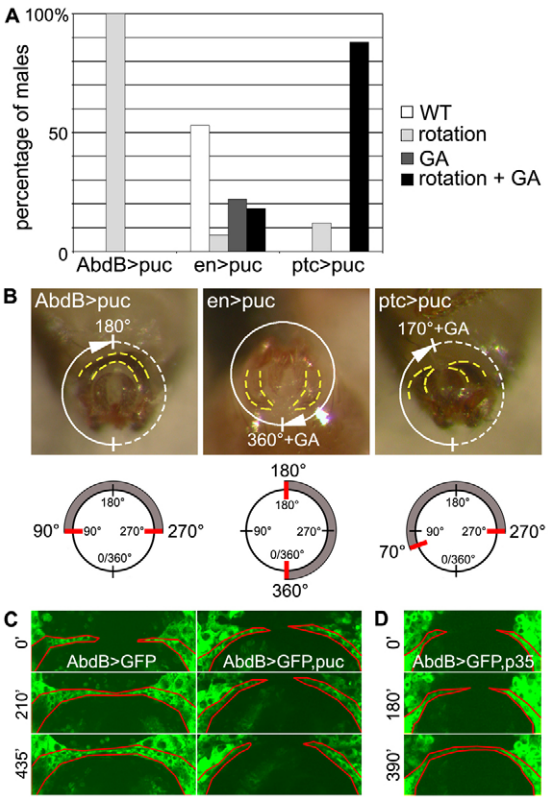

Fig. 5. JNK controls dorsal fusion of the A8 segment and genital arch formation. (**A**) Percentages of genital plate defects of adult males overexpressing *puc* with *AbdB-GAL4* (*n*=274), *en-GAL4* (*n*=140) or *ptc-GAL4* (*n*=148). Four categories can be distinguished: WT, rotation defects, genital arch fusion defects (GA) and defects affecting both events. (**B**) Examples of these defects and diagrams showing degrees of rotation associated with each genotype. 100% of the *AbdB-GAL4/UAS-puc* males (left panel) underwent incomplete rotation (between 90 and 270°, picture shows a 180° rotation) with correct arch fusion. Genital plates of *en-GAL4/+;UAS-puc/+* males (middle panel) rotated 180-360° with or without arch fusion (picture shows a full rotated plate with arch defects). For *ptc-GAL4/+;UAS-puc/+* plates (right panel), rotation stopped between 70 and 270°, mostly with arch fusion defects (picture shows a 170° rotation associated with absence of genital arch fusion). Yellow dotted lines delineate the dorsal part of the genital arch. (**C**) Still images from Movie 1 in the supplementary material showing the dorsal part of genital discs. Genital plate of an *AbdB>GFP* (*UAS-GFP/SM5;AbdB-GAL4/TM6B*) pupa has everted and the A8 segment is in progress of closure (left panel). Rotation starts once closure has finished. Co-expression of Puc (*UAS-GFP/+;AbdB-GAL4/UAS-puc*) inhibits closure of the A8 segment, but rotation starts nonetheless, before aborting (right panel). (**D**) Still images from Movie 2 in the supplementary material showing the correct dorsal fusion of a genital plate overexpressing the apoptosis inhibitor *p35* (*UAS-GFP/UAS-p35;AbdB-GAL4/+*). Red outlines enclose the limits of the A8. Green, GFP. Time in minutes is indicated on the left of each still image.

obtained by overexpressing a dominant-negative form of Bsk. In addition, we never observed sinistral rotation owing to perturbation in JNK activity, going against a role the JNK pathway in left–right asymmetry establishment like myosin ID (R.R., J.-B. Coutelis and A. Petzoldt, unpublished data). Taken together, these data indicate that JNK activity is required in the A8 segment for full rotation of the male genital plate, as well as in the A9 for the correct fusion of the genital arch.

In order to better comprehend JNK-regulated genital plate formation, we developed live imaging of the male pupal disc undergoing rotation. *AbdB-GAL4*-driven expression of GFP enabled live visualization of the A8 segment of the male disc (Fig. 5C; see Movie 1 in the supplementary material). During metamorphosis of the genital disc, the A8 segment first flattens and then encloses the A9 and A10 segments (Keisman et al., 2001). We observed that, before the onset of rotation, the two lateral ends of the A8 segment have not yet encircled entirely the A9 and A10 tissues (Fig. 5C, left panels; see Movie 1 in the supplementary material). They progressively migrate towards each other and then meet. It is only when they have fused dorsally that rotation can occur. Interestingly, overexpression of *puc* in the A8 segment inhibits this fusion (Fig. 5C, right panels; see Movie 1 in the supplementary material). Despite this, rotation starts, but is incomplete, which gives rise to the adult phenotype described in Fig. 5B. This process of tissue sealing is analogous to other JNK-dependent epithelial sheet movements like DC of the embryo, thorax closure of the wing discs and wound healing. The merger also taking place dorsally in the male genital disc we named dorsal fusion of the male genital disc (not to be confused with genital arch fusion). Previous studies suggested that apoptosis promotes rotation and genital arch formation possibly through JNK signalling (Abbott and Lengyel, 1991; Macias et al., 2004; McEwen and Peifer, 2005). For example, suppression of apoptosis by overexpression of the caspase inhibitor *p35* mimics the defects observed in plates overexpressing *puc* (Macias et al., 2004; McEwen and Peifer, 2005). However, our results strongly suggest that this is not the case for the dorsal fusion of the A8 segment, as *p35* expression specifically in the A8 has no effect on its closing (Fig. 5D; see Movie 2 in the supplementary material). Like embryonic DC, JNK probably induces changes in cell morphology without triggering cell death. In conclusion, we show that JNK activity is required for complete rotation of the male genital plate by controlling closure of the A8 segment.

scaf acts as an antagonist of JNK signalling

As previously mentioned, we noticed that *scaf* loss of function in the embryo (Fig. 3C) did not lead to holes in the dorsal part of the cuticle like the ones due to mutations in positive regulators of the JNK pathway. Rather, *scaf* mutations induced holes in the head resembling to the ones associated with *anterior open* (*aop*) mutations, as well as puckering of the dorsal cuticle also observed in *puc* mutants, two genes that negatively regulate JNK activity (Martin-Blanco et al., 1998; Riesgo-Escovar and Hafen, 1997). Ectopic activation of JNK in the embryonic epidermis by expression of either the active (hep^{act}) or the wild-type form of *hep* gave rise to similar anterior open and puckered phenotypes (Fig. 6A). Thus, the *scaf* phenotypes might be due to hyperactivity of JNK signalling, suggesting that, like *puc* and *aop*, *scaf* might antagonize the activity of the JNK pathway.

The *puc-lacZ* staining and the effect of Puc expression in the imaginal disc (Figs 4, 5) suggest that, like in the embryo, JNK signalling needs to be precisely controlled for proper male genital plate morphogenesis. Hence, JNK hyperactivity should also trigger plate malformation. To address this question, we overexpressed *hep* during male genital disc development. The active form of *hep* induced lethality with all the drivers that were tested; therefore, we used the wild-type form, which allowed the eclosion of adult flies. Like for *scaf* loss-of-function, the male

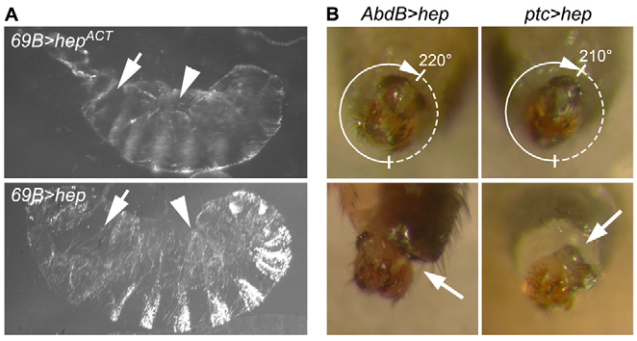

Fig. 6. JNK gain-of-function phenotypes resemble *scaf* loss-of-function phenotypes. (**A**) Ectopic activation of the JNK pathway in *69B>hep^{act}* (*UAS-hep^{act}/+;69B-GAL4/+*; top panel) or *69B>hep* (*69B-GAL4/UAS-hep*; bottom panel) embryos led to cuticles with openings in the anterior part (arrows) and puckering in the dorsal part (arrowheads), like for *scaf* mutant embryos (see Fig. 3C). (**B**) Ectopic activation of JNK signalling in *AbdB>hep* (*AbdB-GAL4/UAS-hep*; left panels; 29°C) or *ptc>hep* (*ptc-GAL4/+;UAS-hep/+*; right panels) male genital discs induced defects like the ones observed in discs with reduced *scaf* activity (see Fig. 4B), such as incomplete rotation (top panels) and separation of the plate from the abdomen (arrows; bottom panels).

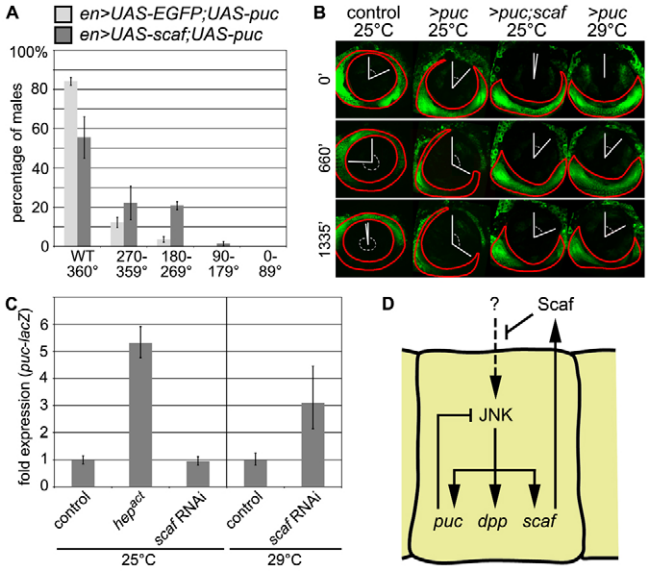

Fig. 7. *scaf*, a novel antagonist of JNK activity. (**A**) Co-expression of Scaf aggravated the genitalia rotation defects caused by Puc overexpression. The *en-GAL4* driver was used to co-express *puc* and *GFP* as a control (light gray bars) or *puc* and *scaf* (dark gray bars). Results are presented as percentages of male plates showing WT rotation or incomplete rotation in 90° decrements. Error bars correspond to s.d. (3 replicates) and a Wilcoxon test indicated a highly significant difference between the two conditions with $P<0.001$. (**B**) Still images from Movie 3 in the supplementary material showing dorsal fusion and rotation of genital discs. Four conditions were tested: control at 25°C (*UAS-GFP/SM5;AbdB-GAL4/TM6B*), *>puc* at 25°C or 29°C (*UAS-GFP/+;AbdB-GAL4/UAS-puc*) and *>puc; scaf* at 25°C (*UAS-GFP/UAS-scaf;AbdB-GAL4/UAS-puc*). At 25°C, the defects of dorsal fusion and rotation were more severe with *scaf* co-expression and resembled the ones seen at 29°C with *puc* expression alone. Red outlines enclose the limits of the A8, whereas the vertical white line indicates the dorsal position of the disc and the other line follows rotation. Green, GFP. (**C**) Quantitative PCR showing an increase of the JNK target gene *puc* (*puc-lacZ*) in *scaf* RNAi embryos (*pnr-GAL4,puc^{E69}/UAS-scafRNAi,UAS-Dicer*) raised at 29°C. Relative fold expression (set to 1 for the controls) showed a temperature-dependent augmentation of th RNAi effect. As a positive control, we used embryos in which JNK activity is increased (*UAS-hep^{act}/+;pnr-GAL4,puc^{E69}/+*; raised at 25°C). Relative expression minimum and maximum values (error bars) were calculated according to the algorithm of 95% confidence level (StepOne software). (**D**) Model of *scaf* function as an inducible antagonist of JNK activity. Like *puc* and *dpp*, *scaf* expression depends on the JNK pathway. Whereas Puc negatively regulates the JNK pathway in a cell autonomous manner, Scaf might act in the extracellular space to control JNK signalling during epithelium morphogenesis (see text).

escapers displayed misrotation defects and plate malformations, showing that excess JNK activity is also detrimental to genital plate formation (Fig. 6B).

To further confirm the negative action of *scaf*, we co-expressed Scaf along with Puc in the genital disc with *en-GAL4*. We observed that *scaf* enhanced the effect of *puc*, as rotation was more incomplete with Puc and Scaf expression compared with Puc and GFP (Fig. 7A). This result was confirmed by live-imaging of the A8 dorsal fusion. Indeed, the A8 extremities did not migrate dorsally when Scaf was co-expressed at 25°C, increasing the defect observed with Puc expression alone at the same temperature (Fig. 7B; see Movie 3 in the supplementary material). Consistently, this severe phenotype resembles the one seen when Puc overexpression is enhanced at 29°C (Fig. 7B; see Movie 3 in the supplementary material). This corroborates the effect of Scaf overexpression on adult male genital plates described above and validates *scaf* as a negative regulator of JNK-controlled epithelial morphogenetic movements.

Scaf could act directly by restraining JNK signalling activity, behaving as an inducible antagonist of the pathway, or indirectly by affecting another event (i.e. another pathway). To test the former possibility, we used quantitative PCR on *scaf* RNAi embryos (*pnr-GAL4,puc-lacZ>scafRNAi*) and measured the level of *puc-lacZ* expression. Although no difference with the control was observed at 25°C, *scaf* loss-of-function at 29°C induced an increase of *puc* expression in the LE (Fig. 7C), indicating that JNK activity was upregulated. In conclusion, our work shows that *scaf* regulates the JNK pathway, acting in a negative-feedback loop during epithelial morphogenesis.

DISCUSSION

We isolated *scaf* in a genome-wide microarray screen aiming at identifying new JNK target genes in the *Drosophila* embryo (R.R., F. Carballès and S.N., unpublished data). Here, we showed that *scaf* is specifically induced by the JNK pathway in the LE cells that drive embryonic DC. To our knowledge, this is the third gene, after *dpp* and *puc*, showing this very specific site of expression under the control of JNK. In addition, we demonstrated that *scaf* expression is regulated by JNK in the A8 segment of the male genital disc. Scaf is also detected in the JNK-responsive cells (expressing *puc-lacZ*) of wing and leg discs (R.R., unpublished data), indicating that *scaf* can be considered as a general JNK target gene during epithelial morphogenesis. We determined that, like other proteins of the SP family, Scaf is a secreted SPH. Importantly, our results point to a negative role of *scaf* against JNK activity during DC in the embryo and during male terminalia formation in the pupa. Therefore, in addition to the inducible antagonist *puc*, the JNK pathway restrains its own activity during epithelial morphogenesis through the expression of the SPH gene *scaf*.

The amount of trypsin- and chymotrypsin-like SP enzymes in metazoan genomes is highly variable, from a dozen in *Caenorhabditis elegans* to more than two hundred in dipteran species like *Drosophila melanogaster* and about a hundred in mammals (Pils and Schultz, 2004). Gene expansion that occurred in flies is remarkable and concerns both the active enzymes and their homologues, indicating specific adaptations to environment and life strategies. Catalytic domains of SP enzymes share high structural similarities and substrate specificity is insured by a binding cleft located near the active site, as well as surface loops present in the SP domain (Perona and Craik, 1995; Perona et al., 1997). SPH proteins have lost their catalytic activities and it is assumed that they have adopted new functions based on novel binding capacities (Pils and Schultz, 2004). For instance, SPH could compete with an active SP for specific substrates.

Classical genetics has revealed the implication of various genes in DC (Harden, 2002; Noselli and Agnes, 1999) and other studies have identified several JNK target genes (Glise et al., 1995; Glise and Noselli, 1997; Homsy et al., 2006; Jasper et al., 2001; Munoz-Descalzo et al., 2005; Thomas et al., 2009). However, *scaf* is the first member of the SP family with a role in this epithelial sealing movement. Like for the *Drosophila* SPH gene *mas* (Murugasu-Oei et al., 1996; Murugasu-Oei et al., 1995), mutations in *scaf* did not show complete expressivity and penetrance in the embryo. One straightforward explanation is the presence of a redundant protein among the various other SPH of the *Drosophila* genome. Compensatory mechanisms, which are known to be important during DC (Hutson et al., 2003), could also hide the impact of *scaf* removal. Nevertheless, our results showed that *scaf* is important for morphogenesis by directly modulating the activity of the JNK pathway. How *scaf* negatively acts is still an open question, but it is probable that Scaf plays a role in the extracellular space, in contrast to the strong intracellular inhibitor Puc (see model in Fig. 7D). The signal that activates JNK signalling (and therefore DC) has not yet been discovered, preventing a straightforward analysis of Scaf molecular action. SP proteins are well-described for their role in activating signal transduction pathways or in degrading the extracellular matrix (ECM) (Lopez-Otin and Matrisian, 2007), and defects in muscle attachment observed in *mas* mutations might be due to a decrease in cell-matrix adhesion (Murugasu-Oei et al., 1995). Accordingly, possible roles of Scaf could be to act locally on an unknown extracellular signal or at the level of the putative receptor of the JNK pathway, through interaction with the ECM. Functioning in a negative-feedback loop, *scaf* would allow a fine tuning of signalling in JNK-active tissues.

The JNK signalling pathway is a major player of epithelial morphogenesis in many organs and developmental stages and its activity must be precisely controlled to coordinate tissue sealing. Two JNK target genes, *puc* and *scaf*, code for antagonists and therefore participate in this control. Whereas Puc acts intracellularly, Scaf is likely to operate in the extracellular space and represents the first secreted regulator of JNK-dependent epithelial sealing. Further studies of the role of *scaf* will highlight how a signal transduction pathway synchronizes collective cell behaviour in a three-dimensional environment, and how these cell rearrangements are controlled extracellularly to lead to a precise coordination of the movement.

Acknowledgements
We thank R. Mann, A. Brand, E. Sanchez-Herrero, N. Perrimon, K. Basler, the Bloomington Drosophila Stock Center (http://flystocks.bio.indiana.edu/bloomhome.htm), the Vienna Drosophila RNAi Center (VDRC; http://www.vdrc.at/) and the Exelixis Collection (https://drosophila.med.harvard.edu/) for fly stocks; the Drosophila Genomics Resource Center (DGRC; https://dgrc.cgb.indiana.edu/) for the *scaf* EST, as well as Developmental Studies Hybridoma Bank (DSHB; http://dshb.biology.uiowa.edu/) for antibodies. We are grateful to A. Petzoldt and J.-B. Coutelis for help in dissecting male genital discs and for dissections of adult male genital plates; to D. Cerezo for help in recombinant screening; to R. Delanoue for help in Q-PCR; to F. De Graeve and S. Schaub for help in statistical analyses; and to laboratory members for helpful discussions. Work in the S.N. laboratory is supported by CNRS, ANR, ARC, CEFIPRA, EMBO Yip and FRM.

Competing interests statement
The authors declare no competing financial interests.

Supplementary material
Supplementary material for this article is available at
http://dev.biologists.org/lookup/suppl/doi:10.1242/dev.050781/-/DC1

References

Abbott, M. K. and Lengyel, J. A. (1991). Embryonic head involution and rotation of male terminalia require the *Drosophila* locus head involution defective. *Genetics* **129**, 783-789.
Anderson, K. V. (1998). Pinning down positional information: dorsal-ventral polarity in the *Drosophila* embryo. *Cell* **95**, 439-442.
Bates, K. L., Higley, M. and Letsou, A. (2008). Raw mediates antagonism of AP-1 activity in *Drosophila*. *Genetics* **178**, 1989-2002.
Bonin, C. P. and Mann, R. S. (2004). A piggyBac transposon gene trap for the analysis of gene expression and function in *Drosophila*. *Genetics* **167**, 1801-1811.
Byars, C. L., Bates, K. L. and Letsou, A. (1999). The dorsal-open group gene raw is required for restricted DJNK signaling during closure. *Development* **126**, 4913-4923.
Casso, D., Ramirez-Weber, F. and Kornberg, T. B. (2000). GFP-tagged balancer chromosomes for *Drosophila melanogaster*. *Mech. Dev.* **91**, 451-454.
Chen, E. H. and Baker, B. S. (1997). Compartmental organization of the *Drosophila* genital imaginal discs. *Development* **124**, 205-218.
Davie, E. W., Fujikawa, K. and Kisiel, W. (1991). The coagulation cascade: initiation, maintenance, and regulation. *Biochemistry* **30**, 10363-10370.
Delaney, J. R., Stoven, S., Uvell, H., Anderson, K. V., Engstrom, Y. and Mlodzik, M. (2006). Cooperative control of *Drosophila* immune responses by the JNK and NF-kappaB signaling pathways. *EMBO J.* **25**, 3068-3077.
Estrada, B., Casares, F. and Sanchez-Herrero, E. (2003). Development of the genitalia in *Drosophila melanogaster*. *Differentiation* **71**, 299-310.
Fernandez, B. G., Arias, A. M. and Jacinto, A. (2007). Dpp signalling orchestrates dorsal closure by regulating cell shape changes both in the amnioserosa and in the epidermis. *Mech. Dev.* **124**, 884-897.
Franke, J. D., Montague, R. A. and Kiehart, D. P. (2005). Nonmuscle myosin II generates forces that transmit tension and drive contraction in multiple tissues during dorsal closure. *Curr. Biol.* **15**, 2208-2221.
Freeland, D. E. and Kuhn, D. T. (1996). Expression patterns of developmental genes reveal segment and parasegment organization of *D. melanogaster* genital discs. *Mech. Dev.* **56**, 61-72.
Glise, B. and Noselli, S. (1997). Coupling of Jun amino-terminal kinase and Decapentaplegic signaling pathways in *Drosophila* morphogenesis. *Genes Dev.* **11**, 1738-1747.
Glise, B., Bourbon, H. and Noselli, S. (1995). hemipterous encodes a novel *Drosophila* MAP kinase kinase, required for epithelial cell sheet movement. *Cell* **83**, 451-461.
Harden, N. (2002). Signaling pathways directing the movement and fusion of epithelial sheets: lessons from dorsal closure in *Drosophila*. *Differentiation* **70**, 181-203.
Holland, P. M., Suzanne, M., Campbell, J. S., Noselli, S. and Cooper, J. A. (1997). MKK7 is a stress-activated mitogen-activated protein kinase kinase functionally related to hemipterous. *J. Biol. Chem.* **272**, 24994-24998.
Homsy, J. G., Jasper, H., Peralta, X. G., Wu, H., Kiehart, D. P. and Bohmann, D. (2006). JNK signaling coordinates integrin and actin functions during *Drosophila* embryogenesis. *Dev. Dyn.* **235**, 427-434.
Hutson, M. S., Tokutake, Y., Chang, M. S., Bloor, J. W., Venakides, S., Kiehart, D. P. and Edwards, G. S. (2003). Forces for morphogenesis investigated with laser microsurgery and quantitative modeling. *Science* **300**, 145-149.

Jasper, H., Benes, V., Schwager, C., Sauer, S., Clauder-Munster, S., Ansorge, W. and Bohmann, D. (2001). The genomic response of the *Drosophila* embryo to JNK signaling. *Dev. Cell* **1**, 579-586.
Kambris, Z., Brun, S., Jang, I. H., Nam, H. J., Romeo, Y., Takahashi, K., Lee, W. J., Ueda, R. and Lemaitre, B. (2006). *Drosophila* immunity: a large-scale in vivo RNAi screen identifies five serine proteases required for Toll activation. *Curr. Biol.* **16**, 808-813.
Keisman, E. L., Christiansen, A. E. and Baker, B. S. (2001). The sex determination gene doublesex regulates the A/P organizer to direct sex-specific patterns of growth in the *Drosophila* genital imaginal disc. *Dev. Cell* **1**, 215-225.
Kiehart, D. P., Galbraith, C. G., Edwards, K. A., Rickoll, W. L. and Montague, R. A. (2000). Multiple forces contribute to cell sheet morphogenesis for dorsal closure in *Drosophila*. *J. Cell Biol.* **149**, 471-490.
Lopez-Otin, C. and Matrisian, L. M. (2007). Emerging roles of proteases in tumour suppression. *Nat. Rev. Cancer* **7**, 800-808.
Macias, A., Romero, N. M., Martin, F., Suarez, L., Rosa, A. L. and Morata, G. (2004). PVF1/PVR signaling and apoptosis promotes the rotation and dorsal closure of the *Drosophila* male terminalia. *Int. J. Dev. Biol.* **48**, 1087-1094.
Martin-Blanco, E., Gampel, A., Ring, J., Virdee, K., Kirov, N., Tolkovsky, A. M. and Martinez-Arias, A. (1998). puckered encodes a phosphatase that mediates a feedback loop regulating JNK activity during dorsal closure in *Drosophila*. *Genes Dev.* **12**, 557-570.
McEwen, D. G. and Peifer, M. (2005). Puckered, a *Drosophila* MAPK phosphatase, ensures cell viability by antagonizing JNK-induced apoptosis. *Development* **132**, 3935-3946.
Munoz-Descalzo, S., Terol, J. and Paricio, N. (2005). Cabut, a C2H2 zinc finger transcription factor, is required during *Drosophila* dorsal closure downstream of JNK signaling. *Dev. Biol.* **287**, 168-179.
Murugasu-Oei, B., Rodrigues, V., Yang, X. and Chia, W. (1995). Masquerade: a novel secreted serine protease-like molecule is required for somatic muscle attachment in the *Drosophila* embryo. *Genes Dev.* **9**, 139-154.
Murugasu-Oei, B., Balakrishnan, R., Yang, X., Chia, W. and Rodrigues, V. (1996). Mutations in masquerade, a novel serine-protease-like molecule, affect axonal guidance and taste behavior in *Drosophila*. *Mech. Dev.* **57**, 91-101.
Nakamura, T., Nishizawa, T., Hagiya, M., Seki, T., Shimonishi, M., Sugimura, A., Tashiro, K. and Shimizu, S. (1989). Molecular cloning and expression of human hepatocyte growth factor. *Nature* **342**, 440-443.
Noselli, S. and Agnes, F. (1999). Roles of the JNK signaling pathway in *Drosophila* morphogenesis. *Curr. Opin. Genet. Dev.* **9**, 466-472.
Perona, J. J. and Craik, C. S. (1995). Structural basis of substrate specificity in the serine proteases. *Protein Sci.* **4**, 337-360.
Perona, J. J., Tsu, C. A., Craik, C. S. and Fletterick, R. J. (1997). Crystal structure of an ecotin-collagenase complex suggests a model for recognition and cleavage of the collagen triple helix. *Biochemistry* **36**, 5381-5392.
Pils, B. and Schultz, J. (2004). Inactive enzyme-homologues find new function in regulatory processes. *J. Mol. Biol.* **340**, 399-404.
Polaski, S., Whitney, L., Barker, B. W. and Stronach, B. (2006). Genetic analysis of slipper/mixed lineage kinase reveals requirements in multiple Jun-N-terminal kinase-dependent morphogenetic events during *Drosophila* development. *Genetics* **174**, 719-733.
Rawlings, N. D. and Barrett, A. J. (1993). Evolutionary families of peptidases. *Biochem. J.* **290**, 205-218.
Reed, B. H., Wilk, R. and Lipshitz, H. D. (2001). Downregulation of Jun kinase signaling in the amnioserosa is essential for dorsal closure of the *Drosophila* embryo. *Curr. Biol.* **11**, 1098-1108.
Reed, B. H., Wilk, R., Schock, F. and Lipshitz, H. D. (2004). Integrin-dependent apposition of *Drosophila* extraembryonic membranes promotes morphogenesis and prevents anoikis. *Curr. Biol.* **14**, 372-380.
Ricos, M. G., Harden, N., Sem, K. P., Lim, L. and Chia, W. (1999). Dcdc42 acts in TGF-beta signaling during *Drosophila* morphogenesis: distinct roles for the Drac1/JNK and Dcdc42/TGF-beta cascades in cytoskeletal regulation. *J. Cell Sci.* **112**, 1225-1235.
Riesgo-Escovar, J. R. and Hafen, E. (1997). *Drosophila* Jun kinase regulates expression of decapentaplegic via the ETS-domain protein Aop and the AP-1 transcription factor DJun during dorsal closure. *Genes Dev.* **11**, 1717-1727.
Ring, J. M. and Martinez Arias, A. (1993). puckered, a gene involved in position-specific cell differentiation in the dorsal epidermis of the *Drosophila* larva. *Dev. Suppl.* 251-259.
Ross, J., Jiang, H., Kanost, M. R. and Wang, Y. (2003). Serine proteases and their homologs in the *Drosophila melanogaster* genome: an initial analysis of sequence conservation and phylogenetic relationships. *Gene* **304**, 117-131.
Shah, P. K., Tripathi, L. P., Jensen, L. J., Gahnim, M., Mason, C., Furlong, E. E., Rodrigues, V., White, K. P., Bork, P. and Sowdhamini, R. (2008). Enhanced function annotations for *Drosophila* serine proteases: a case study for systematic annotation of multi-member gene families. *Gene* **407**, 199-215.
Speder, P. and Noselli, S. (2007). Left-right asymmetry: class I myosins show the direction. *Curr. Opin. Cell Biol.* **19**, 82-87.
Speder, P., Adam, G. and Noselli, S. (2006). Type ID unconventional myosin controls left-right asymmetry in *Drosophila*. *Nature* **440**, 803-807.
Srivastava, A., Pastor-Pareja, J. C., Igaki, T., Pagliarini, R. and Xu, T. (2007). Basement membrane remodeling is essential for *Drosophila* disc eversion and tumor invasion. *Proc. Natl. Acad. Sci. USA* **104**, 2721-2726.
Thibault, S. T., Singer, M. A., Miyazaki, W. Y., Milash, B., Dompe, N. A., Singh, C. M., Buchholz, R., Demsky, M., Fawcett, R., Francis-Lang, H. L. et al. (2004). A complementary transposon tool kit for *Drosophila melanogaster* using P and piggyBac. *Nat. Genet.* **36**, 283-287.
Thomas, C., Rousset, R. and Noselli, S. (2009). JNK signalling influences intracellular trafficking during *Drosophila* morphogenesis through regulation of the novel target gene Rab30. *Dev. Biol.* **331**, 250-260.
Wada, A., Kato, K., Uwo, M. F., Yonemura, S. and Hayashi, S. (2007). Specialized extraembryonic cells connect embryonic and extraembryonic epidermis in response to Dpp during dorsal closure in *Drosophila*. *Dev. Biol.* **301**, 340-349.
Wu, H., Wang, M. C. and Bohmann, D. (2009). JNK protects *Drosophila* from oxidative stress by trancriptionally activating autophagy. *Mech. Dev.* **126**, 624-637.
Xu, H., Brill, J. A., Hsien, J., McBride, R., Boulianne, G. L. and Trimble, W. S. (2002). Syntaxin 5 is required for cytokinesis and spermatid differentiation in *Drosophila*. *Dev. Biol.* **251**, 294-306.